Acta Phys. Hung. A 19/1 (2004) 000–000

HEAVY ION PHYSICS

Data Quality and First Science Results of the Pierre Auger Experiment

A. Etchegoyen[1]

[1] Laboratorio Tandar, CNEA and CONICET, Buenos Aires, Argentina

Received 1 January 2004

Abstract. The Pierre Auger Project is building an ultra high energy cosmic ray observatory in the Province of Mendoza, Argentina. A description of the detectors will be given with an emphasis in their hybrid design and calibration and first data will be shown.

Keywords: high energy cosmic rays, new facility, Cherenkov detectors and telescopes, first data.
PACS: 95.55.Vj, 95.85.Ry, 29.40.Ka

1. Introduction

The Pierre Auger Project studies the highest energies known in nature which are cosmic rays arriving at the top of the atmosphere with both galactic and extragalactic origin. It is designed to measure the energy spectrum and the arrival direction of cosmic rays with energies above 3×10^{18} eV and to statistically identify the mass composition of the primary cosmic ray particle. At these energies the primary particle entering the top of the atmosphere produces an airshower composed of a large number of secondaries and therefore the airshower detectors are designed to sample either the longitudinal or lateral shower profiles.

Auger aims at building two observatories, one in each hemisphere. In 2000 the construction of the austral observatory started in the Province of Mendoza, Argentina and construction will be finished by the end of 2006. Augers two distinct features are its exceptional size and its hybrid nature, which are respectively imposed by the low flux at the highest energies and the need for accurate experimental measurements. Auger [1] spans over an area of $3,000 km^2$ and is constituted by 24 fluorescence detector telescopes (18 working) and 1600 surface detectors (1,000 installed). The telescopes have a field of view (FOV) of 30^0 in azimuth and 30^0 in

1219-7580/04/ $ 20.00

elevation and they are installed in 4 telescope buildings, each one hosting 6 telescopes. A layout of the observatory is shown in Fig. 1.

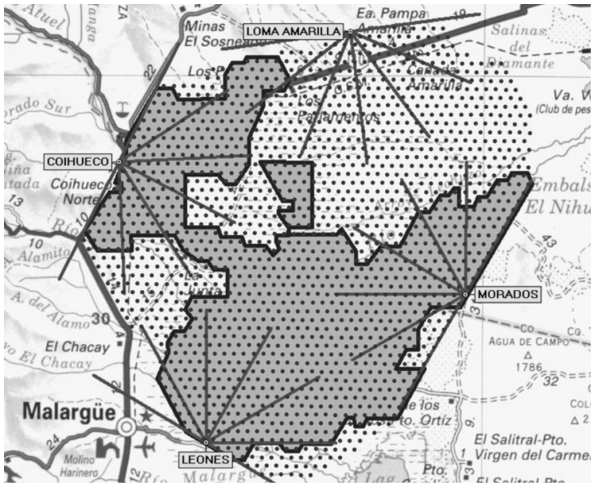

Fig. 1. Auger Observatory layout showing the four telescope sites with the 30^0 FOV lines. Dots represent surface detectors and in dark grey is the area of those already deployed.

Several experiments were performed since the first detection of a cosmic ray shower with ascribed energy in excess of 10^{20} eV at Volcano Ranch in 1962. Cosmic ray experiment use surface detectors (SD) deployed over a chosen area in order to sample the shower secondary particles lateral profile, see for instance the Akeno

Giant Air Shower Array (AGASA,http://www.icrr.u-tokyo.ac.jp/as/as.html). One single experiment, Flys Eye/HiRes (see http://www.cosmic-ray.org/), make use of fluorescence detectors (FD)which sample the longitudinal shower profile by detecting the atmospheric nitrogen fluorescence light produced by excitations by shower electrons. SD arrays have a 100 % duty cycle and make use of simulations in order to evaluate the energy, while FDs have a 10-15 % duty cycle (clear, dark nights) but do not resort to simulations for the energy estimation, although they rely on both the atmospheric fluorescence yield and on a continuous evaluation of the atmospheric light attenuation length. The aperture is well defined for SD at higher energies where the trigger efficiency is unitary and it is calculated with Monte Carlo simulations for FD. They are clearly two systems that complement each other.

2. The Surface Array

The SD array consists of 1600 cylindrical water Cherenkov detectors of $10m^2 \times 1.2m$ arranged on a triangular grid with 1.5 km spacing covering $3,000km^2$. This spacing is justified since shower lateral profiles extend for several square kilometers (area increasing with shower energy) and therefore it suffices to place detectors some hundreds of meter away from each other in order to collect signal densities as a function of the distance to the shower axis. SDs have successfully been employed in Australia, Bolivia, Germany, Italy, Japan, Russia, Tibet, United Kingdom, and United States.

The SD operation principle is based on the Cherenkov light produced by charged shower secondaries (and gammas after pair production)when traversing the 12 t of pure waterlodged in the tank. This light illuminates the tank (see Fig. 2) interior which is covered with a laminated Tyvek (excellent diffused reflectivity) with black plastic (water and external light barrier). Part of the light is collected by three 9" photo multipliers tubes (PMT) placed at the water surface, then amplified and digitized by the electronics and sent to the Central Station via telecommunications. The system is powered with solar panels and batteries and the timing is done with a GPS signal.

A tank absolute energy calibration is needed to measure the Cherenkov energy deposited in each detector by shower secondaries in order to reconstruct the shower parameters (in particular the primary particle energy). The main advantage of water Cherenkov tanks is their large muon signal, since shower muons have both a large energy and are not stopped in the tank by bremsstrahlung. Therefore background muons can be used to perform accurate, remote, fast and automatic SD calibrations. They are currently performed every 6 minutes for monitoring purposes and also 150,000 count histograms are raised and stored per station triggered by an airshower. Background muons produce histograms with a hump close to the average charge collected when a tank is fully traversed by a single high-energy muon impinging vertically at the center (VEM, Vertical Equivalent Muon, adopted as the tank calibration unit)[2], as seen in Fig. 3. This robust calibration is quite

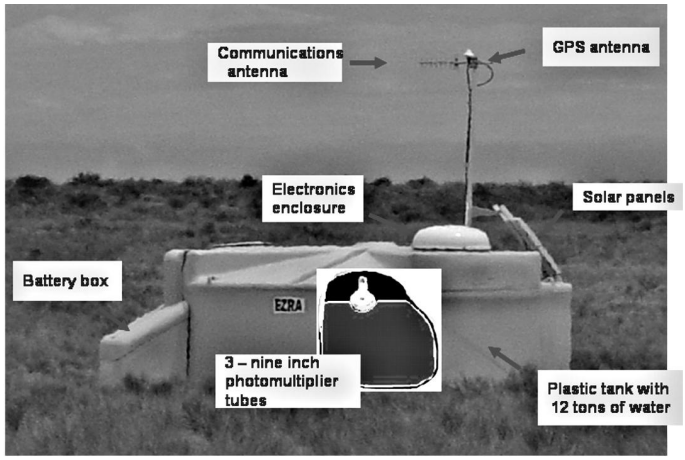

Fig. 2. An Auger surface detector

instrumental in order to obtain reliable experimental data. Note for instance that Auger works with ambient temperatures fluctuating $\sim 20^0$/day (see Fig. 3) and the VEM unit was measured to follow these fluctuations [1], given rise to a 10% variation in the trigger rate. Auger dynamic VEM value corrects this uncertainty on line given a flat trigger rate over time.

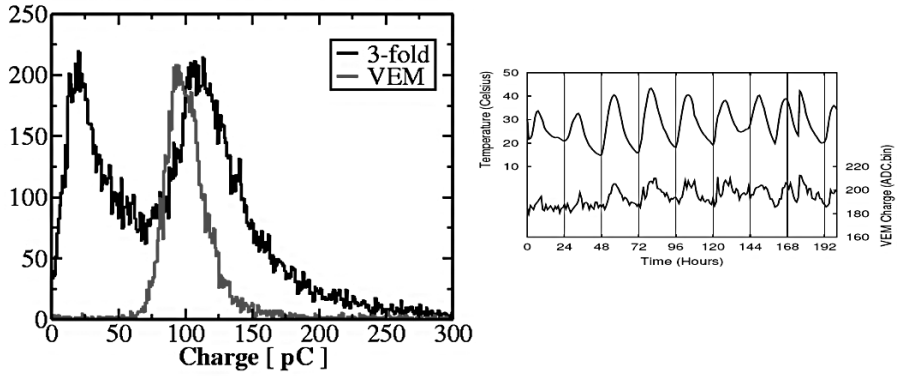

Fig. 3. lhs: hump histogram (black) raised by requiring a 3-fold coincidence of the three tank PMTs and VEM histogram (grey) raised with a triple coincidence among a top and bottom centered scintillators and the tank; rhs: temperature and VEM charge fluctuations over time.

The SD Performance is quite satisfactory at the moment being on-time 94% of the time. The array will be detecting 1,500 events/year when finished. A typical event will be shown in a latter section.

3. The Fluorescence Telescopes

The Observatory altitude was chosen so that shower particle densities at ∼1 km from the ground will be near their maximum value in their longitudinal development. The FD telescopes will therefore measure the shower development until it is detected at the atmospheric depth of the Observatory, i.e. when it reaches the ground.

Auger telescopes (see Fig. 4) have adopted a Schmidt optics [3], since it is free of coma aberration. The shower profile, as it develops in the atmosphere, is sequentially seen by adjacent PMTs, each of them with a FOV of $1.5^0 \times 1.5^0$ in azimuth and elevation, respectively. The fluorescence light enters through a diaphragm with an annular Schmidt lens corrector ring (corrects outer rays shperical/coma aberrations [4]) and it is reflected from a $3.5 \times 3.5m$ spherical segmented mirror onto the phototube camera. The PMTs are surrounded by a simplified version of Winston cones to enhance light collection at phototube edges.

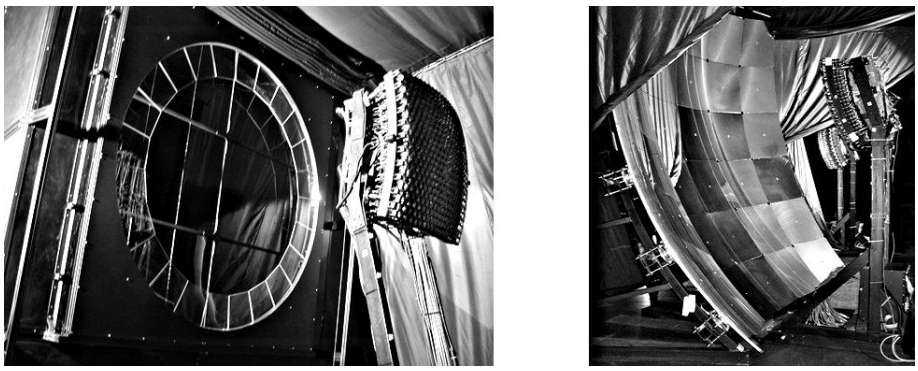

Fig. 4. lhs: diaphragm with corrector ring and the 440 phototube camera; rhs: spherical mirror and camera.

A full calibration of the telescopes implies to obtain from the flash ADC counts the number of shower electrons, i.e. an absolute calibration to derive the number of photons at the telescope diaphragm from the phototube signal (drum calibration, [5]) and a measurement of the atmospheric light attenuation to derive the number of photons at the shower axis from those at the diaphragm (mainly based on LIDAR systems, [6]).

The end-to-end calibrations uses a 2.5 m diameter, 1.4 m deep drum-shaped diffuse light source which mounts at the telescope diaphragm. The wall and back

of the drum are covered with Tyvek while the front face is a 0.38 mm thick Teflon sheet. The light flux at the diaphragm is measured at the laboratory. In this fashion and from a single measurement the calibration for each pixel (phototube) is obtained, which is in average ~ 5 photons/ADC channel.

The atmospheric monitoring is performed with a variety of methods: backscatter LIDAR systems, cloud cameras, star monitors, and meteorological stations at each FD site, three horizontal attenuation monitors with a light source in an FD site and a receiver in another one, and a steerable laser system placed near the center of the array (Central Laser Facility, CLF). Also a number of meteorological radiosonde launchings is performed in order to know the atmospheric conditions dependance on altitude. Auger relies heavily on the elastic backscatter LIDAR systems, two of which are currently operational. They perform routine aerosol sky observations on an hourly basis and, for airshowers of particular interest, the FD informs the shower geometry to the LIDAR and requests a "shoot-the-shower" procedure by which the LIDAR shoots along the shower arrival direction for real-time aerosol information.

The above-mentioned CLF [7] consists in a steerable UV laser from which part of the calibrated pulsed light is sent to a nearby surface detector system. In this fashion, CLF shoots can simulate a hybrid detection since the laser diffused light will be detected by the FDs and simultaneously the diverted light by the tank. The CLF provides i) FD and hybrid geometry and energy reconstructions, ii) SD-FD clock stability with time, and iii) aerosol profiles in the CLF-FD direction.

The hybrid detection is of paramount importance to drastically reduced the systematic uncertainties in the shower geometry reconstruction, i.e. the core position and the arrival direction (see Fig. 5).

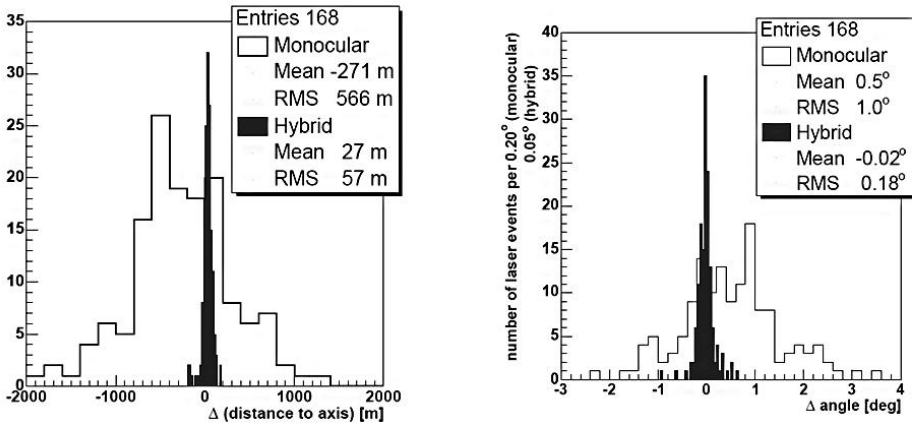

Fig. 5. Hybrid (shaded histogram) and FD (background histogram) geometrical reconstructions of laser shots.

It is seen from the figure that the uncertainties both in core position and arrival direction reconstructions are reduced by an order of magnitude when the FD reconstruction is complemented with a single tank information. Note that the laser shots geometry is known, since the core position is where the laser sits and the direction is where it points. The geometry reconstruction is performed by the relative time at which the PMTs trigger. Generally, the curve of the PMT trigger-time dependance on the PMT-shower axis angle (pixel angle χ) is not curved enough as to obtain from the fit the three requested parameters without large uncertainties, several parameter sets would reproduce data. The subjacent problem is that all FD PMTs trigger in a short period of time. This uncertainty might be solved by including a corresponding tank trigger-time since it will occur at a later time, providing in this manner a much better geometry reconstruction, as seen in the figure.

As a concluding remark of the previous two sections it is said that the SD and FD systems were described with emphasis in the extreme care taken in the calibration of these instruments, which allows a reliable reconstruction of airshowers.

4. Data Analyses

As was mentioned in the previous section, the airshower geometry reconstruction is based on PMT triggering timing and this actually applies to all data (hybrid, FD, and SD data). On the other hand, the energy is estimated from the longitudinal and/or lateral profiles (see Fig. 6).

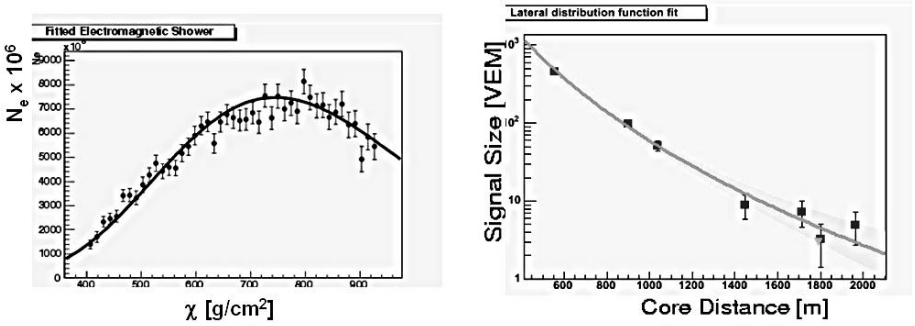

Fig. 6. Longitudinal (lhs) and lateral (rhs) profiles of a hybrid event.

Fig. 6 shows a hybrid event which triggered an FD and seven tanks. The event reconstruction gave $E \simeq 80EeV$ ($1EeV = 10^{18}eV$) and zenithal arrival angle $\Theta \simeq 30^0$. The fluorescence technique estimates the event energy by integration of the longitudinal profile [8]. A full lateral profile integration is not convenient for the SD technique since the bast majority of the particles is close to the core from where there is no experimental data. It has long been recognized [9] that the particle density

at large core distances is a good energy estimator. The actual distance is obtained by taken into account shower-to-shower fluctuations (mainly atmospheric depths of first interactions), core position and lateral distribution function uncertainties. It also depends on assumptions about the hadronic interaction model and the primary cosmic ray composition. For Auger, this distance is taken as 1,000 m, and therefore the surface array energy estimator is S(1000), the signal at that distance.

4.1. The Cosmic Ray Spectrum

As it was mentioned in the Introduction, the Auger energy scale is based on fluorescence measurements since they do not rely on simulations. Hybrid events are used to calibrate S(1000) in energy and this calibration is then applied to SD events since the surface array has a 100% duty cycle and a fixed aperture at high energies. Such a calibration is of course done with hybrid events and the current one is shown in Fig. 7.lhs.

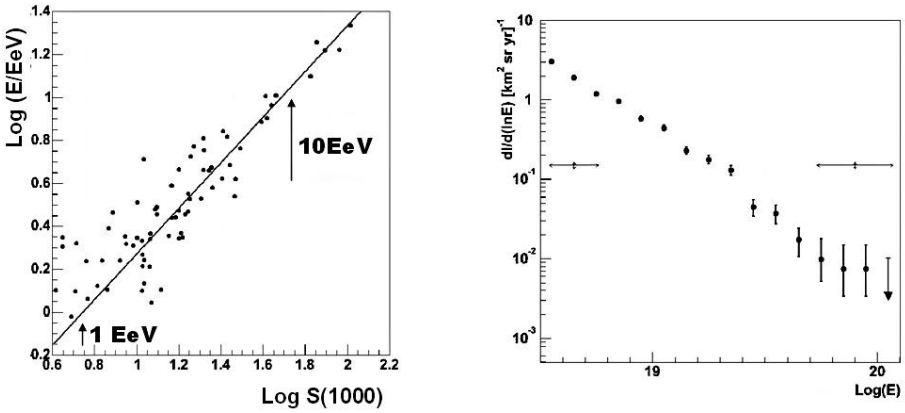

Fig. 7. lhs: S(1000) energy calibration with fluorescence telescope energy, rhs: Auger preliminary spectrum

An Auger preliminary spectrum is shown in Fig. 7.rhs where the FD systematic uncertainties plus those arising from the calibration functional form (uncertainty increasing with energy due to the reduced number of events) are estimated and plotted for two energy regions, 3.0 and 100 EeV ($\sim$ 30 and 50%), respectively. Therefore a better understanding and reduction of systematic uncertainties is necessary prior to undertake a meticulous study of the two main spectrum features in this energy range, the ankle and the GZK cut-off [8].

4.2. Anisotropy Searches Near the Galactic Center

There has been long suspected and indirectly found experimentally that between $10^{17} - 10^{19}$ eV the origin of cosmic rays change from galactic to extragalactic. The obvious acceleration site in our galaxy is its center since it is by far the most energetic region. It harbors, for instance, a super-massive black hole (Sgr A*, 2,600,000 solar masses). The gamma ray telescope HESS, placed in Namibia, has detected an excess γ ray emission of energies of up to 10 TeV from the galactic center region [10]. Supernova remnants (possible high energy cosmic ray accelerators) peak near the galactic center, and for instance, Sgr A East is speculated [11] to be a candidate for acceleration of heavy ions and neutrons with energies in excess of 1.0 EeV. Neutrons at such energies can reach the earth from the center of the galaxy without decaying. Since they travel undeflected by the pervading magnetic fields, an extrapolation of their arrival direction will point backwards to any existing anisotropy near the galactic center. Localizing such a source would be an unambiguous and direct evidence supporting the galactic origin of these sort of cosmic rays. Auger, being a southern hemisphere observatory, is perfectly placed to undertake a detailed study of the galactic center.

Two experiments, AGASA (Japan) and SUGAR (Australia) have reported an excess of cosmic rays near the galaxy center [12, 13]. AGASA reports a 4.5σ excess with energies in the range 1-2.5 EeV in a 20^0 radius region and SUGAR a 2.9σ excess in 5.5^0 radius region with energies 0.8 - 3.2 EeV. Auger has a nearly uniform exposure in this region of interest and it has detected 1155 (three times more than AGASA) to be compared to 1161 events of an isotropic flux, that is a ratio 1.00 ± 0.03. In the SUGAR smaller circle Auger detected 144 events (SUGAR $\times$ 10) out of 151 expected, i.e. a ratio 0.95 ± 0.08. Therefore, Auger detects no excess failing to confirm the anisotropies previously reported.

4.3. Exotic Processes

Highest energy cosmic rays may not necessarily be produced by an acceleration mechanism (bottom-up models). Their origin could be from the decay of super massive particles with masses very much in excess of 10^{20} eV (top-down models). Typical top-down models include decays of gauge bosons from topological defects of the early universe, decays of a super massive component of dark matter, and the so-called Z-burst scenario, in which a large fraction of these cosmic rays are decay products of Z bosons produced in the scattering of ultrahigh energy neutrinos on cosmological relic neutrinos. The comparison between the observed and predicted spectra constrains the mass of the heaviest neutrino. A common feature of these processes is that a large fraction of the highest energy cosmic ray primaries would be photons and neutrinos.

Auger can detect and tag neutrinos [14] by measuring very inclined showers, since they could be identified as very penetrating showers. As such they might reach the detectors before the electromagnetic component attenuates completely. Typical

primaries (heavy ions, nucleons, and gammas) generate showers on entering the atmosphere and due to the large volume of atmosphere traversed by nearly horizontal showers, only their muonic shower component reaches the detectors. These showers with no electromagnetic component are customary referred as old showers. Therefore, young very inclined showers are a clear indication of neutrino primaries. Also earth skimming τ neutrinos which convert in the Earths crust and produce a τ initiated shower on exiting the earth could be also identified as young showers slightly pointing upwards.

Gamma primaries can be identified since their longitudinal profile develops deep in the atmosphere. They will also have a reduced number of muons as secondaries. Sixteen hybrid events with $E > 10^{19}$eV were studied [15]. Several simulations assuming gamma primaries were performed for each event taking its reconstructed energy and geometry with their uncertainties as simulation inputs. In this fashion, a distribution of the atmospheric depth at which each shower reaches it maximum is obtained. It is then evaluated the probability that the experimental atmospheric depth at shower maximum corresponds to a photon primary. For this Auger data sample, an upper limit on the photon fraction of 26%, confidence level 95% was obtained (see Fig. 8). Still, the exotic processes become important at higher energies, $E \geq 30EeV$, so this photon bound is limited by both the reduced statistics and the relatively low energy for these processes.

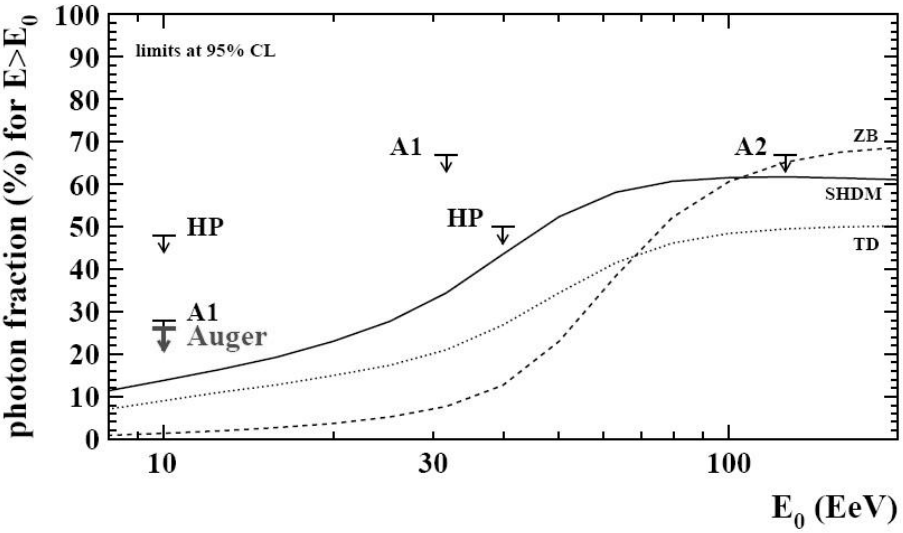

Fig. 8. Upper limits at 95% CL for gamma primaries for different experiments. Theoretical predictions from [16]

5. Conclusions

The hybrid method and the calibration of both FD and SD systems have been outlined with an effort to clarify the significant strength of the Auger Observatory for elucidating the main current topics of interest of high energy cosmic ray astrophysics. Preliminary Auger data have been presented outlining the science of the project. Auger is working well within the design parameters and in a few years the science outcome of the project will be based on very high quality data of statistical significance.

References

1. Auger Collaboration, J. Abraham et al., *Nucl. Inst. and Meth.* **A 523** (2004) 50-95.
2. A. Etchegoyen, P. Bauleo, X. Bertou, C.B. Bonifazi, A. Filevich, M.C. Medina, D.G. Melo, A.C.Rovero, A.D. Supanitsky, A. Tamashiro (for the Pierre Auger Collaboration), *Nucl. Inst. and Meth.* **A 545** (2005) 602-612; M. Aglietta et al. (for the Pierre Auger Collaboration), *Proceeding of the 29th International Cosmic Ray Conference Pune (2005).*
3. A. Cordero, E. Cantoral, J. Castro, A. Fernandez, and R. Pastrana, *Auger Technical Note.* GAP-96-039 (1996).
4. R. Sato, C.O. Escobar (for the Pierre Auger Collaboration), *Proceeding of the 29th International Cosmic Ray Conference*, Pune (2005).
5. P. Bauleo, J. Brack, L. Garrard, J. Harton, R.Knapik, R. Meyhandan, A.C. Rovero, A. Tamashiro, and D. Warner (for the Pierre Auger Collaboration), *Proceeding of the 29th International Cosmic Ray Conference*, Pune (2005).
6. R. Cester et al. (for the Pierre Auger Collaboration),*Proceeding of the 29th International Cosmic Ray Conference*, Pune (2005).
7. F. Arqueros et al. (for the Pierre Auger Collaboration), *Proceeding of the 29th International Cosmic Ray Conference*, Pune (2005).
8. M. Nagano and A.A. Watson, *Rev. Mod. Phys.* **72** (2000) 689-732.
9. M. Hillas, *Acta Phys. Acad. Sci. Hung* **29**, Suppl 3, 355.
10. F. Aharonian et al. (The HESS Collaboration), *Astron. Astrophys.* **425** (2004) L13.
11. D. Grasso and L. Maccione, *astro-ph/0504323* (2005).
12. N. Hayashida et al. (The AGASA Collaboration), *Astroparticle Phys.* **10** (1999)303.
13. J.A. Bellido, R.W. Clay, Br.R. Dawson, and M. Johnston-Hollitt, *Astroparticle Phys.* **15** (2001)167.
14. X. Bertou et al., *Astroparticle Phys.* **17** (2002)183.
15. M. Risse (for the Pierre Auger Collaboration), *Proceeding of the 29th International Cosmic Ray Conference* Pune (2005).
16. G. Gelmini, O.E. Kalashev, and D.V. Semikoz, *astro-ph/0506128* (2005).